International Journal of Applied Engineering Research
ISSN 0973-4562 Volume 10, Number 3 (2015) pp. 6693-6711

http://www.ripublication.com

Hybrid Continuous Wavelet Genetic Fuzzy Neural Exponential Probability Density Function Based Translation-Invariant Contourlet Transform For Denoising In Medical Images

C.S.Manikandababu[1] and Dr. N.J.R. Muniraj[2]

[1]Assistant Professor (Selection Grade)/ECE, [2]Principal
[1]Sri Ramakrishna Engineering College,
[2]Tejaa Shakthi Institute of Technology for Women
Coimbatore, Tamil Nadu INDIA
[1]E-mail: c.smanikandababu@yahoo.com

ABSTRACT

Digital Imaging and Communication in Medicine (DICOM) is a well accepted standard mainly employed for the purpose of accumulation and transmission of the medical images. Medical images take part a significant role in analysis, treatment and investigation. Roughly all the outputs of the Magnetic Resonance (MR), Ultrasonography (US), Digital Subtraction Angiography (DSA) and Computerized Tomography (CT) are stored as DICOM format, Elimination of noise from this format happen to be a continuous challenge. The objective of this research work is to build a novel two stage denoising methods to eliminate noises from medical images model which includes two major phases: wavelet decomposition and Translation Invariant Contourlet Transform (TIC). The algorithm begins with globally denoising the DICOM image samples with the help of the hybrid continuous wavelet genetic fuzzy neural exponential probability density function based translation-invariant contourlet transform denoising and it is named as CWGFNEPDF-TIC. In the proposed method, at the beginning the wavelet coefficients are calculated by Exponential Probability Density Function (EPDF) to eliminate noise from medical image samples. Wavelets are a collection of functions in order that multiple resolution nature of wavelets offers a natural frame work for the examination of time series. The estimated wavelet coefficients are forecasted by Genetic Fuzzy Neural Network (GFNN). The potential of this network to approximate functions from specified input-output medical images data and it has exploited the localization feature of a wavelet to concentrate on local properties. The proposed approach is evaluated with the help of 3D medical image data. The simulation results demonstrate that the model is capable of producing a

reasonable accuracy along with better Peak Signal to Noise Ratio (PSNR), Mean Square Error (MSE), Root Mean Square Error (RMSE), Structural Similarity Index (SSIM) and Normalized Cross-Correlation (NXC).

Keywords: Medical Image Processing, Exponential Probability Density Function (EPDF), Wavelet Transform (WT), Continuous Wavelet transform (CWT), Contourlet Transform (CT), Translation-Invariant Contourlet Transform (TICT), Digital Imaging and Communication in Medicine (DICOM), Fuzzy Neural Network (FNN), Peak Signal to Noise Ratio (PSNR), Mean Square Error (MSE).

Introduction

Digital images take part a considerable role in routine applications [1]. Even though the production technology of the electronic equipments such as digital cameras, camera phones, etc has been considerably developed, the captured images still undergo quite a lot of distortions. In the midst of several distortions, noise is one of the most considerable, and can be introduced by some sources such as: the recording medium film, digital sensor, transmission medium and dimension and quantization errors [2]. The strength of impulse noise has the tendency of being either fairly raised or low down. As a result, it could harm the image quality rigorously and cause certain loss of image information details [3]. Because of additive white Gaussian noise which can be influenced by deprived image acquisition or by transmitting the image data in noisy communication channels, distortion is one of the most widespread scenarios. Impulse and speckle noises are also additional categories of noises [1]. The image acquires a mottled, gritty, textured or snowy look with the existence of noise. Consequently, while attempting to recover an original image from noisy image, an overwhelming concentration has been observed in the current years [4]. The dispute of eliminating the noise from images has a robust history [4]. As an effect, with the purpose of constructing a quantitative post-processing more strong and well-organized, image processing procedures often demand eliminating image artifacts at earlier stage [5].

Medical images are the imperative constituent of any electronic medical record. Volume of these medical images is extremely enormous and the electronic medical record also takes incredibly large space to accumulate. Therefore, it becomes complicated to share such type of enormous quantity images through the network and it also consumes lot of time to transmit a medical image. Hence, DICOM standard assists to supervise enormous quantity of data necessary for medical imaging. DICOM standard also assists for safe and well-organized sharing of images at the time of sharing patient data. It increases the protection, reliability and consistency of medical image archives retained for legal and agreement purposes.

The amount of medical images generated in the planet is continuously mounting. Enormous amount of three dimensional medical images (3D) are generated every year to identify or observe a therapeutic consequence. They offer data on the form and performance of body organs. Adversely, these data are exceptionally complicated to make use in a quantitative and objective approach. The applications of three-

dimensional reconstruction are abundant and diverged: they broaden from medicine, geography to the shipbuilding. In case of medicine, normally in the biomedical, reconstruction addresses the areas: anatomy, electron microscopy and confocal, radiology of surgery, cell biology, etc... 3D reconstruction is predominantly accepted in microscopy. Certainly, the microscope allows to observe extremely small structures however adversely offers only flat image. On the other hand, tissues, cells or subcellular structures comprise a three-dimensional structural design that the microscope cannot make it. The biologist is consequently deprived of some information. The scanning electron microscope surpasses this setback but it is deficient in flexibility and is imperfect in certain cases. These images are frequently influenced by random noise takes place at some point in the acquisition process. Furthermore, medical images comprised of low-contrast objects are a most important challenge for biomedical scientists. The noise exceedingly influences the visual interpretation of medical images, however also most of the segmentation or clustering approaches. As a result, denoising medical images is an imperative pre-step for medical image investigation.

Noise reduction is an essential process for any approaches, in computer vision and image processing [4]. Image denoising is one of the conventional setbacks in image processing, and has been investigated for a number of years owing to its significant part in several applications. Its objective is to eliminate noise and/or counterfeit details from a specified corrupted image at the same time maintaining its significant characteristics. Image denoising discovers applications in areas such as astronomy in which the resolution inadequacies are rigorous, in medical imaging where the physical necessities for 2 high quality imaging are required for analyzing images of specific events, and in forensic science where potentially constructive photographic indication is sometimes of exceedingly dreadful quality.

Denoising is indispensable and the preliminary step to be taken earlier than the image data is analyzed. It is fundamental to implement an efficient denoising approach, to balance such data corruption. The attempt of image denoising is to enhance an image that is cleaner than its noisy examination. As a result, a significant technology in image examination is noise reduction and the preliminary step to be taken earlier than images is analyzed [6]. Denoising of images is typically done with the subsequent process: The image is converted into some domain in which the noise component is predictable without any complicatedness, to eradicate the noise, a thresholding operation is then implemented, and at last to rebuild a noise-free image.

Wavelet denoising has completely focussed on the exploitation of orthogonal or bi-orthogonal wavelets as a consequence of their reconstructive properties. On the other hand, no specific wavelet has been recognized as being the ‘most excellent’ for denoising. It is commonly known that wavelets having a linear-phase, or close to linear-phase, reaction are desirable, and this has enabled the use of the ‘symlet’ series of wavelets and bi-orthogonal wavelets. A setback with wavelet shrinkage denoising is that the DWT is not translation invariant. When the signal is relocated by one data point the wavelet coefficients do not just move by the equivalent amount. They are totally variant, for the reason that there is no redundancy in the wavelet representation. As a result, the outline of the reconstructed signal following wavelet

shrinkage and transform inversion will be based on the translation of the signal - evidently this is not very adequate.

Wavelets are numerical functions characterized over a specific interval and having an average value of zero that convert data into different frequency components, signifying each component with a resolution corresponding to its scale [7]. The fundamental conception behind the wavelet transform is to characterize any arbitrary function as a superposition of a collection of such wavelets or basis functions. These basis functions are regarded as the baby wavelets and these baby wavelets are derived from a single prototype wavelet recognized as the mother wavelet by means of dilations or contractions (scaling) and translations (shifts) [7]. Wavelets are not best in obtaining the two-dimensional singularities exist in images. As a result, numerous transforms have been proposed for image signals that have integrated directionality and multiresolution and therefore, possibly will more resourcefully obtain edges in natural images. Contourlets [6] are some popular examples. The contourlet transform is one of the novel geometrical image transforms, which can professionally characterize images containing contours and textures [8].

In case of the medical field, images exploited for the diagnosis development takes part a noteworthy role. As a result, denoising which eliminates noise from images is an imperative step in medical image processing. With the intention of accurately condensing noises from 3D medical images and surpass the setback of the wavelet transformation methods, in this research work a novel hybrid Continuous Wavelet Genetic Fuzzy Neural Exponential Probability Density Function based Translation-Invariant Contourlet Transform (CWGFNEPDF-TIC) denoising is proposed, in which the wavelet coefficient function $x(t)$ are computed in accordance with the EPDF and subsequently wavelet transform coefficient values are forecasted to Genetic Fuzzy Neural Network (GFNN). The angular decomposition is given by a Directional Filter Bank (DFB), a second stage of CWGFNEPDF-TIC. The proposed TI version of a subsampled Filter bank obtained through the CWGFNEPDF gives a tight frame in case when the original subsampled FB has a tight frame. Using the proposed CWGFNEPDF together with employing modified versions of the DFB, initiate the TI Contourlet Transform (TICT). The simulation observations show that the proposed CWGFNEPDF-TIC denoising methods is competitively provides best noise removal results than the existing transformation approaches such as Wavelet Transform (WT) and Contourlet Transform (CT) based on the Peak signal to noise ratio (PSNR), Mean Square error (MSE), Root mean square error (RMSE), Structural Similarity Index (SSIM) and Normalized Cross-Correlation (NXC) values for the mentioned images. TICT algorithm to improve the speed of the algorithm, the perform refinement phase the most important wavelet coefficients are first encoded, and it has got a good compression performance.

Background Study

A wide range of research methodologies is utilized for the denoising process on medical image is discussed here. The reviewed researches are categorized depending on the denoising process on several kinds of images such as Radiography, Ultrasound,

MRI and CT images.

Giakos et al., [9] have provided the design of a high-effectiveness optical polarimetric system for imaging of cracks and structural flaws of a rotating metallic shaft. The experimental results have noticeably pointed out that high signal-to-noise ratio signals were achieved, so that it diminished the utilization of processing techniques.

Pierre Gravel et al., [10] have formulated a scheme to investigate the statistical features of the noise exist in several medical images. The scheme was completely intended for categories of noise with uncorrelated fluctuations. Commonly in the physical processes of imaging more willingly than in the tissue textures, such signal fluctuations has been initiated. In order to corrupt medical images, several categories of noise has been contributed; the overall noise was usually presumed to be additive with a zero-mean, constant-variance Gaussian distribution. On the other hand, based on peripheral parameters associated with the image acquisition protocol, statistical analysis has recommended that the noise variance was better modelled by a nonlinear function of the image intensity.

Using DWT, Arivazhagan et al., [1] has tentatively assessed the performance of an Image Denoising System for four levels of DWT decomposition, i.e., Speckle noise added two facial and two CT images. Based on their inclusive experiments carried out with the expanded image denoising software for diverse noise parameters and for various levels of DWT decomposition by utilizing soft thresholding technique, the subsequent decisions were obtained: (i) The maximum PSNR (dB) was accomplished for first level of DWT decomposition (SNR1) for the majority of the images appended with Speckle noise, (ii) Additionally, it was found that the SNR accomplished for superior level of DWT decomposition was smaller than SNR1 or SNR2 and for the fourth level of DWT decomposition, rigorous blurring takes place, irrespective of images and noise constraints and (iii) Also, it was interested to observe that for images distorted with minor noise densities, single level of DWT decomposition was adequate; at the same time for images distorted with higher noise densities irrespective of images second level of DWT decomposition was adequate.

3D wavelet transform for MRI denoising is formulated by

Yang Wang et al., [11] for Rician noise elimination. Owing to delineating ability of wavelet, 3D WT was utilized to offer efficient representation of the noisy coefficients. Bilateral filtering of the approximation coefficients in a modified neighborhood enhanced the denoising effectiveness and successfully preserved the significant edge features. In the meantime, the detailed subbands were processed with an improved NeighShrink thresholding approach. Validation was carried on both simulated and genuine clinical data. With the help of the Peak Signal-to-Noise Ratio (PSNR) to compute the quantity of noise of the MR images, here achieved an average PSNR enhancement of 1.32 times with simulated data.

A great remarkable quality of the wavelet transform is its ability to protect detail at various scales, owing to its capability to model the information nearby exist in the image as a result of the multiresolution decomposition [12].

Pizurica et al., [13] formulated the filtering by means of the DWT. It exploits the information that MR magnitude image observes a Rician distribution and diffusion method such as Perona-Malik's, but settled in to the Rician distribution, has been

formulated in [14]. In this scenario, the square of the amplitude image is also exploited, correcting the bias and employing a bilateral filter (Gaussian filtering in the spatial and amplitude domains) over approximation coefficients (it is also depends on the Rician image distribution).

Image denoising indicates the enhancement of a digital medical image that has been distorted by Additive White Gaussian Noise (AWGN). The digital medical image or video can be distorted by several kinds of noises, such as, impulse noise, Poisson noise and AWGN. The term "image or video is de-noising" is typically dedicated to the difficulty associated with AWGN. In order to solve the AWGN difficulty, a Discrete Wavelet Transform (DWT) is investigated for medical image denoising is presented in [15]. In the beginning, the AWGN is created randomly and appended to the input medical image. The noisy medical images are decomposed by DWT at different levels.

Junmin Deng et al., [16] developed a CT image denoising method which integrates Curvelet transformation with Monte-Carlo algorithm; initially CT image's Curvelet decomposition is carried out. Then, Monte-Carlo algorithm is exploited to approximate high frequency coefficients. At last, the coefficients are shrunk based on the threshold function. It has the demerit of deprived directionality, which has undermined its practice in several applications.

An integration of the total variation minimization approach and the wavelet scheme denoising algorithm has been formulated by YangWang et al., [17] for medical images. Although preserving sharpness of objects, they have demonstrated that their approach gives efficient noise removal in real noisy medical images. In addition, their approach allows implementing an efficient automatic stopping time criterion extensively.

Rajeesh et al., [18] developed the denoising of Magnetic Resonance Images using wave atom shrinkage. They have found that compared to wavelet and curvelet shrinkages, this approach had realized a better SNR. A specific benefit of this method is the edge preserving feature. Furthermore, the efficiency of this method will be highlighted by comprising a huge dataset of real-time normal and pathological MR images.

Proposed Methodology

In this research work, developed a denoising methods for developing a Translation-Invariant Contourlet (TIC) approach from a general multidimensional and multichannel subsampled Filter Bank (FB) for 3D medical image samples. Specifically, the proposed methods are expanded from general continuous wavelet transform in the company of exponential distribution function which is appropriate to a general multidimensional subsampled filter bank. In the proposed wavelet transform based Translation-Invariant contourlet transformation scheme includes of two phases: At first CWT values are estimated depending on exponential distribution function and continuous wavelet transform values are forecasted to Genetic Fuzzy Neural Network (GFNN), consequently the proposed wavelet transform is called as CWGFN and it is integrated to TIC method, then it is called as CWGFNEPDF-TIC. The proposed TI

version of a subsampled filter bank obtained through the CWGFNEPDF offers a tight frame when the original subsampled FB has a tight frame. With the help of the proposed CWGFNEPDF together with employing modified versions of the DFB, establish the TI Contourlet Transform (TICT). Regardless of the effectiveness of the proposed TICT for image denoising [19] is more feasible for image processing applications. The proposed approach assists in denoising of DICOM images. The comprehensive organization of the proposed medical image denoising for DICOM images is illustrated in the following Fig.1.

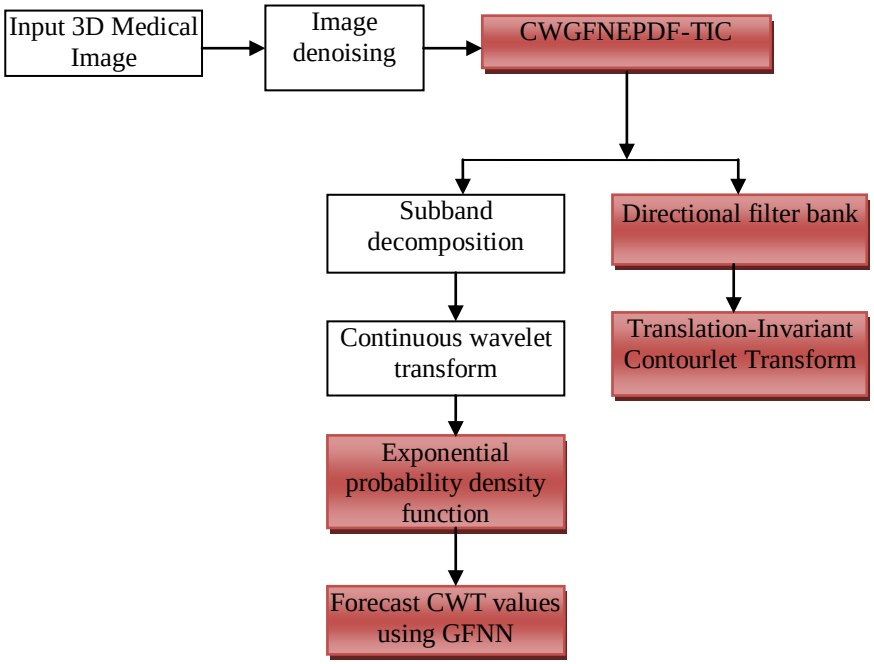

Figure 1: Structural representation of the proposed medical image denoising using DICOM images

Hybrid continuous wavelet fuzzy neural exponential probability density function Based Translation-Invariant contourlet for Image denoising

In the proposed approach, contrary to the Laplacian pyramid exploited in TIC, two phases have been included in the system in which the initial phase enables for breakdown of the DICOM image into subbands. Computation of the wavelet coefficient functions for continuous wavelet transformation function having subbands for each DICOM input images are also carried out in this phase. In this phase, the decomposed values of noise level in the continuous wavelet coefficients are forecasted to fuzzy neural network. The angular decomposition is given by a Directional Filter Bank (DFB), a second phase of CWGFNEPDF-TIC. The separable and non-separable filter banks are been executed in first and second phase correspondingly. Consider I_T represents the true image and N indicates the noise component. As given by Jin et al., [20], the association of noisy image I_N related to I_T

and N can be represented as,

$$I_N = I_T + N \quad (1)$$

Denoising I_N by means of wavelet transform to recover the true signal I_T can be given as,

$$I_R = \sum_i W(I_N, j, t) \quad (2)$$

where I_R signifies the reconstructed signal, W indicates the wavelet based denoising, j indicates the level of decomposition, and t represents the function that intends to eradicate noise elements in the transform domain at the same time conserving the correct signal coefficients. For the entire DICOM input images, the conventional three highpass bands is acquired related to the LH, HL, and HH bands at every level (j),$W(I_N, j, t)$ in the continuous wavelet transformation approaches. The quantity of directions is been reduced at the same time going through the coarser levels $(j < J)$ at every other dyadic scale when preferred utmost number of directions $N_D = 2^L$ on the optimum level of the wavelet transform $J = f(t)$ is been initiated. Consequently, the anisotropy scaling law; condition $width \approx length^2$ may perhaps be attained. The value of $I_N(t)$ is computed by openly giving the input data of any distribution kind and by arbitrarily defining the Square-integrable function $I_N(t)$ at a scale $a > 0$ in the wavelet transformation domain. In this work, distribution function dependent approaches are exploited to compute the values of the $I_N(t)$ in the scale parameter by further taking the shape parameter (slope) into account in order to surpass the complications of the CWT transformation methods. This supplementary consideration of slope results in enhancement of the wavelet transformation outcome than normal Continuous Wavelet Transformation (CWT) outcome by varying the values of the image scale subsequently computation of its decomposition values by means of the following equation:

$$W(I_N, j, t) = \frac{1}{\sqrt{a}} \int_{-\infty}^{\infty} I_N(t) \psi \left(\frac{t-b}{a} \right) dt \quad (3)$$

Where $a > 0, I_N \in (a, b)$. The considered mother wavelet functions are oscillatory bandpass filters in the time domain. Therefore, the fundamental function is a low frequency function seizes a stretched version of the mother wavelet for a bigger values and a contracted version called short-duration, high-frequency function for lesser values. Coefficients of subband $C_i (i = 1, 2, \cdots, j)$ with threshold t_i to acquire the denoised subband C_i'.

$$C_i'(I_T) = \begin{cases} I_T - t_i \; if \; I_T \geq t_i \\ I_T + t_i \; if \; I_T \leq -t_i \\ 0 \quad if \; |I_T| < t_i \end{cases} \quad (4)$$

where the threshold for each subband t_i is worked out with the help of equation 5.

$$t_i = \frac{S\alpha_i^2}{\sigma_i} \quad (5)$$

At this point, σ_i represents the standard derivation for the i^{th} subband and the noise variance for each subband, α_i^2, is calculated with the help of equation 6.

$$\alpha_i^2 = \left[\frac{median\ (C_i)}{0.6745}\right]^2 \quad (6)$$

The scale parameter S is calculated by means of L_m, i.e length of subband at m^{th} scale. Exponential probability density function with continuous wavelet transforms, a translation of the wavelet offers time localization and is characterized by a parameter b. The probability density function (pdf) of an exponential distribution is given as,

$$f(I_N;\lambda) = \begin{cases} \lambda e^{-\lambda I_N} & I_N \geq 0 \\ 0 & I_N < 0 \end{cases} \quad (7)$$

On the other hand, this can be described using the Heaviside step function, $H(I_N)$

$$f(I_N;\lambda) = \lambda e^{-\lambda I_N} H(I_N) \quad (8)$$

At this time $\lambda > 0$ is the Wavelet slope parameter of the distribution, frequently called as the rate parameter. The Heaviside step function, or the unit step function, typically symbolized by H (however from time to time u or θ), is a discontinuous function whose value is 0 for negative argument and 1 for positive argument. I_N represents the wavelet coefficient subband value in equation (4). The transformation is converted into irreversible only when it holds the following admissibility condition,

$$c_\psi = \int_0^\infty \frac{|\Psi(f)|^2}{|f|} df < \infty \quad (9)$$

The above mentioned equation implies that the DC component $\Psi(0)$ have to be disappeared. Accordingly, to offer good time resolution, $\psi(t)$ represents a bandpass signal that should adequately decay quick. The Parseval relation for the wavelet transform is given as follows,

$$\int_{a=0}^{\infty} \int_{b=-\infty}^{\infty} |W(I_N, j, t)|^2 \frac{db\ ba}{a^2} \vDash c_\psi \int_{-\infty}^{\infty} |I_N(t)|^2\ dt \quad (10)$$

The orthonormal wavelet transforms keeps back the energy among the various scales that are parameterized by a in the manner such that,

$$\int_{a=0}^{\infty} |\psi(t)|^2\, dt = \int_{-\infty}^{\infty} \frac{1}{|a|}\, \psi \left|\left(\frac{t-b}{a}\right)\right|^2 dt \quad (11)$$

For the construction of the continuous wavelet transform, the Morlet wavelet happens to be a fine example of a mother function that is given as,

$$\psi(t) = [exp(-2i\pi f_0 t) - exp\ (-2\pi^2 f_0^2 \sigma^2)] exp\ (-\frac{t^2}{2\sigma^2}) \quad (12)$$

Its Fourier transform is given as follows,

$$\psi(f) = \sqrt{2\pi\sigma^2}\{exp[-2\pi^2\sigma^2(f-f_0)^2] - exp(-2\pi^2\sigma^2 f^2)\, exp(-2\pi^2\sigma^2 f_0^2)\} \quad (13)$$

which meets the admissibility condition $\Psi(0) = 0$. By selecting this mother function, the continuous wavelet transform upon time discretization $t = n\Delta T$ turns out to be as below,

$$W(I_N,j,t)=\frac{\Delta T}{\sigma\sqrt{2\pi a}}\sum_{n=-\infty}^{\infty}s(n)\,exp\left[-\frac{(n\Delta T-b)^2}{2a^2\sigma^2}\right]\times exp\left(-2i\pi f_0\frac{n\Delta T-b}{a}\right) \quad (14)$$

where ΔT represents the sampling time in seconds.

In order to examine the wavelet coefficient values from the wavelet transform approaches, the proposed methods commence the Genetic Fuzzy Neural Network (GFNN) to forecast the wavelet coefficient values for assessing time series particularly when it is nonlinear and non-stationary. It holds the advantage of high resolution of wavelets and learning and GFNN. The GFNN algorithm is comparable to the Sugeno controller. At first, the input wavelet coefficient vector outcome from continuous wavelet transform $WY(I_N,j,t)\in\mathbb{R}^{m\times 1}$ is fuzzified by the vector of membership functions in the m distinct property dimensions, $\tilde{f}=(\mu_1,\dots\mu_m)$, $\tilde{f}\colon W(I_N,j,t)\to[0,e]$, in which e indicates the m-dimensional unit vector. The fuzzy vector $\tilde{f}\big(W(I_N,j,t)\big)$ is then combined to a fuzzy signal through a T-norm, i.e., $\propto_p = T\left(\tilde{f}\big(Wx(I_N,j,t)\big)\right)$. In case of necessary, the input wavelet coefficient values can be stated in terms of memberships in each of the linguistic property sets: poor, medium and good. Input m-dimensional pattern $Wx(I_N,j,t)=(Wx_1(I_N,j,t),\dots,Wx_m(I_N,j,t))$ would be signified with a three fuzzifier parameters as given below,

$$\tilde{f}=(\mu_{1,poor},\mu_{1,medium},\dots\mu_{m,good}) \quad (15)$$

In this scenario, the memberships possibly will be suitably signified by the π-function. The vital feature of this approach is the defuzzification of the aggregate signal. The signal $\propto_p$ is initially mapped to each fuzzy output group by a vector $h=(\mu_{G_1},\dots.\mu_{G_k})$ and, at last, aggregated to a crisp group indicator by an appropriate T-conorm,

$$S(c,d)\coloneqq 1-T(1-c,1-d),c,d\in[0,1] \quad (16)$$

This scheme permits condition of separate membership functions for every crisp input and for every fuzzy output group. As a result, the decisive group membership (g_p) for an observation $Wx(I_N,j,t)$ is decided by the following function:

$$g_p=\underset{G_i}{iarg}(S(h(\propto_p)))=\underset{G_i}{iarg}(S(h(T(\tilde{\tilde{f}}(Wx(I_N,j,t))))))) \quad (17)$$

In case if required $\tilde{f}$ is appropriately aggregated over the linguistic properties of the each wavelet coefficients $Wx(I_N,j,t)$,

$$\mathbb{R}^{m\times 1}\ni\tilde{f}=(S\big(\mu_{1,poor},\mu_{1,medium},\mu_{1,good}\big),\dots. \quad (18)$$
$$S(\mu_{m,poor},\mu_{m,medium},\mu_{m,good})$$

In this work, the constituents of the fuzzifier $\tilde{f}$ (primary hidden layer) designate the degree of membership in the fuzzy set superior economic indicators for the equivalent inputs $Wx_i(I_N,j,t);\ i=1,\dots,m$. The mapping function $\tilde{h}$, for a second time, indicates the degree of membership in each of the fuzzy output groups, as activated by the aggregate signal $\propto_p$. In FNN approach the misclassification takes place because the firing level of the fuzzy signal surpasses the point of intersection for the

defuzzifier functions. In case of misclassification, the membership functions in the fuzzifier and defuzzifier are systematically fine-tuned by the GFNN-algorithm, as discussed consequently. The fine-tuning procedure comprises the learning component in the algorithm. With the intention of surpassing the setback of the FNN, employed a genetic algorithm to fine-tune the parameter values of the FNN. Consider $L = 1\ to\ L_{MAX}$ represents the number of the predefined runs and MN indicates the maximum number of the iterations from step 1 to step 4.

Step 0: Indicate the fuzzy membership function in the fuzzifier $\tilde{f}$ for wavelet coefficient and the defuzzifier $(\tilde{h})$. Wavelet coefficient weight value in the fuzzy neural network (FNN), $w = \left(\tilde{f}^{\,MN}, \tilde{h}^{\,MN}\right)$. Consider $mn = 0$ denote the $f(w, C_{mn})$, C_{mn} denote the class and initialize the population.

$$POP(mn) = \begin{bmatrix} w_{1mn} \\ \vdots \\ w_{Nmn} \end{bmatrix} = \begin{bmatrix} (Wx_i(I_N, j, mn), y_{1mn}) \\ \vdots \\ (Wx_i(I_N, j, mn), y_{Nmn}) \end{bmatrix} \quad (19)$$

Where w_{1t} represents the preliminary (weight) value and $w_{it} \in [left, right]$

$$w_{ik} = \begin{cases} w_{ij} + \Delta(mn, right(j) - w_{ik})\ if\ r = 0 \\ w_{ij} + \Delta\left(mn, w_{ik} - left(j)\right)\ if\ r = 1 \end{cases} \quad (20)$$

With

$$\Delta(\mathrm{mn}, \mu) = \mu\alpha\left(1 - \frac{\mathrm{mn}}{\mathrm{MN}}\right)^{\mathrm{b}} \quad (21)$$

$\alpha \in [0,1]$ represents the random variable and b indicates the constant system parameter determining the degree of the mutation operator. $j \in [k+1, k+s]$ the w_{ij} represents accurately rounded (upwards when $r = 0$ and downwards when $r = 1$).

Step 1: Assess the $pop(mn)$ in the ascending organization by means of the $f(w, C_{mn})$. Provide input wavelet coefficients and categorize the samples with the help of FNN. When $\hat{g}_p \neq g_p$ subsequently move to step 2, else move to step 3

Step 2: Consider $\mu_{\hat{g}_p}$ and μ_{g_p} indicates the fuzzy membership function outcome of the false and true results. When $\hat{g}_p \neq g_p$ move to step 3. Else fine-tune the membership function in the fuzzifier $\tilde{f}$ and aggregate the mapping vector $\tilde{h}$.

Step 3: Choose the $\frac{N}{2}$ preeminent individuals from $pop(mn)$ and produce n new individuals in $pop(mn)$ by means of the mixed-integer crossover and non uniform mixed integer mutation.

Step 4: Reiterate the steps 1-3 until convergence $L = L_{MAX}$, subsequently identify the termination criteria as follows: Let $\overline{F_{mn}}$ represent the moving average of the best objective function values derived over a predefined number of the iterations, when $|F_{mn} - \overline{F_{mn}}| < \varepsilon$ then terminate.

Translation-Invariant Contourlet Transform (TICT)

The Directional Filter Bank (DFB) is a most important component of the contourlet transform. It is recognized through iterated quincunx Filter Banks (FBs), and certain resampling operations that simply rearrange coefficients. In a j-level DFB, fragment the frequency space 2^j to wedge-shaped partitions. By means of the noble identities,

one can transmit all sampling operation to the end (start) of the forward (inverse) transform of DFB [21]. Accordingly, one acquires 2^j examination and 2^j synthesis filters, $H_i^{(j)}$ and $G_i^{(j)}$, correspondingly, and the overall sampling matrices $S_i^{(j)}$, as provided below [21]:

$$S_i^{(j)} = \begin{cases} diag\left(2^{j-1}, 2\right), & for\ 1 \le i \le 2^{j-1} \\ diag\left(2, 2^{j-1}\right), & for\ 2^{j-1} \le i \le 2^j \end{cases} \quad (22)$$

In view of the fact that it is the corresponding iterated DFB system for levels, to construct the TI format, it is adequate to hold back the sub sampling operations and multiply the reconstructed signal by a scaling factor, which is for both vertical and horizontal directions. As a result, the redundancy factor of such a format is equivalent to the number of directions. In accordance with the passband sections of the TILP high-pass filters, with the intention of reducing the complexity, for filters and, it is proper to utilize vertically and horizontally oriented DFBs [22], correspondingly. In vertical DFB (VDFB) and horizontal DFB (HDFB) can accomplish predominantly vertical directions and mostly horizontal directions correspondingly. In these two modified DFB approaches, terminate decomposing the signal horizontally or vertically following the first level of the DFB. As a result, the overall sampling matrices for VDFB and HDFB will be,

$$S_i^{(V(t))} = \begin{cases} Q, & for\ subband\ y_1 \\ diag\left(2, 2^{j-1}\right), & for\ 2^{j-1} \le i \le 2^j \\ diag\left(2, 2^{j-1}\right), & for\ 2^{j-1} \le i \le 2^j \\ Q\ \ for\ subband\ y_0 \end{cases} \quad (23)$$

where Q represents the quincunx sampling matrix. In the TI versions of the VDFB and HDFB, have to consider the new sampling matrices to achieve the proper scaling factors. The redundancy factor of the modified (either vertical or horizontal) TIDFB will be $2^{j-1} + 1$.

Experimentation Results

In order to assess the performance of the proposed and existing image denoising methods for DICOM images, the image samples are derived from DICOM sample image sets from http://www.osirix-viewer.com/datasets/. The site includes several number of DICOM samples dataset with different Computerized Tomography (CT), Magnetic Resonance (MR), for 3D backbone DICOM images (Refer Figure 2 (a)) etc. DICOM medical images are denoised by means of denoising approaches. It is necessary to compress using image compression techniques. These image samples results are measured using the parameters like Peak Signal to Noise Ratio (PSNR), Mean Square Error (MSE), Root Mean Square Error (RMSE), Structural Similarity Index (SSIM) and Normalized Cross-Correlation (NXC).

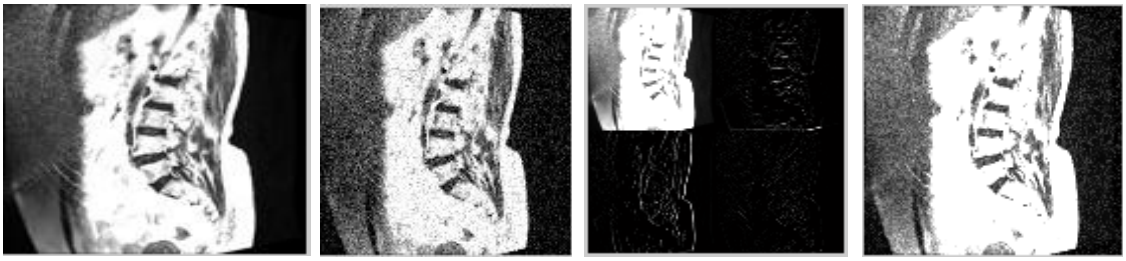

Figure 2 (a) MRI 3D backbone image **Figure 2 (b) Noisy image** **Figure 2 (c) Wavelet image** **Figure 2 (d) Denoised image**

Figure 2 (a) MRI 3D backbone image shows the original image sample , (b) Noisy image shows after the noise are added to images , (c) Wavelet image shows after the wavelet transform is applied to noise image and (d) Denoised image results of the wavelet image

Root-mean-square error (RMSE)

Root-Mean-Square Error (RMSE) is a regularly employed measure of the differences between values predicted by a model or an estimator and the values observed in reality. The RMSD of predicted values $\hat{y}_t$ for times t of a regression's dependent variable y is computed for n different predictions, and it is given as,

$$RMSE = \sqrt{\frac{\sum_{t=1}^{n}(y_t - \hat{y}_t)^2}{n}} \quad (24)$$

Peak Signal to Noise Ratio (PSNR)

Peak signal to noise ratio is characterized as the ratio among the highest possible outcomes results and distorted noise results of the image. The PSNR value for each image is computed with the help of the following formula,

$$PSNR = 10\, log_{10}(MAX_i^2/MSE) \quad (25)$$

MAX_i^2 represents the maximum possible pixel value of the image.

Mean Square Error (MSE)

Mean Square Error (MSE) is characterized as the difference among an estimator results and the true value of the original images results are computed as given below,

$$MSE = \frac{1}{mn}\sum_{i=0}^{m-1}\sum_{j=0}^{n-1}[I(i,j) - K(i,j)]^2 \quad (26)$$

where $I(i,j)$ represents the original image and $K(i,j)$ indicates the approximation to the original image which is also regarded as the decompressed image. M, N represents the image dimensions. The lower value of MSE reveals that the errors are less. Due to inverse relation of MSE and PSNR, the errors will be less when the PSNR is high.

Rationally, signal is the image and noise is the errors generated in the reconstructed image. As a result, when signal to noise ratio is maximum and MSE is less for an image when comparison then one can make a confirmation that this is the better one.

Structural Similarity Index (SSIM)

SSIM considers image deprivation as perceived transformation in structural information. Structural information is the conception that the pixels have strong inter-dependencies particularly when they are spatially near. These dependencies hold significant information regarding the structure of the objects in the visual scene. The SSIM metric is computed on different windows of an image. The measure between two windows x and y of common size $N \times N$ is given below:

$$SSIM(x,y) = \frac{(2\mu_x\mu_y + c_1)(2\sigma_{xy} + c_2)}{(\mu_x^2 + \mu_y^2 + c_1)(\sigma_x^2 + \sigma_y^2 + c_2)} \quad (27)$$

With, μ_x signifies the average of x, μ_y signifies the average of y, σ_x^2 represents the variance of x, σ_y^2 indicates the variance of y, σ_{xy} be the covariance of x and y, $c_1 = (k_1 L)^2\, c_2 = (k_2 L)^2$ are the two variables to stabilize the division with weak denominator; L is the dynamic range of the pixel-values (characteristically this is $2^{\#bits\ per\ pixel} - 1$, $k_1 = 0.01$ and $k_2 = 0.03$) and by default.

Normalized Cross-Correlation (NXC)

Normalized Cross Correlation (NXC) has been frequently exploited as a metric to estimate the degree of similarity (or dissimilarity) among two compared images. The major advantage of the normalized cross correlation over the cross correlation is that it is less susceptible to linear transformations in the amplitude of illumination in the two compared images. In addition, the NCC is confined in the range between –1 and 1. The setting of detection threshold value is much simpler than the cross correlation.

$$NXC(I, \hat{I}) = \frac{\sum_{i=1}^{N}\sum_{j=1}^{M}(I_{i,j}, \hat{I}_{i,j})}{\sum_{i=1}^{N}\sum_{j=1}^{M}(I_{i,j})^2} \quad (28)$$

Table 1 shows the values of performance comparison results of the denoising methods with the parameters like MSE, RMSE and PSNR for DICOM MRI image samples results.

Table 1: DICOM MRI 3D backbone image results

No	MSE (%)			PSNR(dB)			RMSE (%)		
	WT	CT	CWGFNEPDF-TIC	WT	CT	CWGFNEPDF-TIC	WT	CT	CWGFNEPDF-TIC
1	0.76	0.55	0.32	8.56	23.45	28.45	0.89	0.65	0.48
2	0.73	0.51	0.28	12.54	21.45	26.44	0.81	0.63	0.41
3	0.68	0.49	0.27	14.98	20.13	27.46	0.78	0.61	0.38
4	0.78	0.48	0.23	7.56	22.14	30.89	0.81	0.588	0.364
5	0.76	0.52	0.225	9.45	24.87	32.14	0.97	0.564	0.345

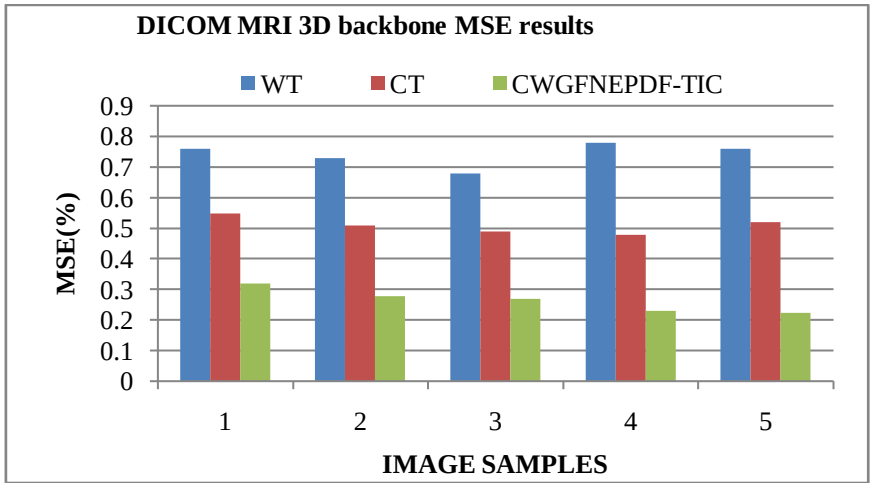

Figure 3: DICOM MRI 3D backbone image samples MSE results

Figure 3 illustrates the MSE results of the DICOM MRI image sample results for samples upto 5 between the Wavelet Transformations (WT), Contourlet Transform (CT) and the proposed CWGFNEPDF-TIC. It shows that the proposed CWGFNEPDF-TIC have lesser MSE results than the existing denoising methods, since the wavelet transformation methods results are forecasted to GFNN, TICT overcomes the problems of CT.

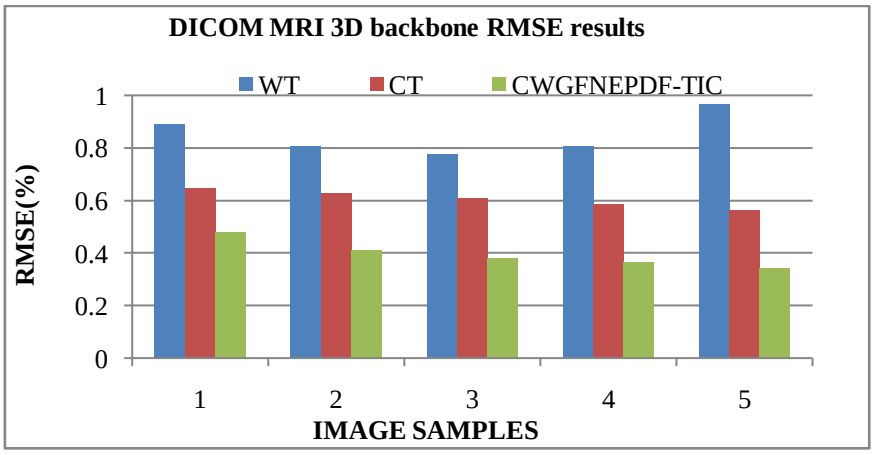

Figure 4: DICOM MRI 3D backbone image samples MSE results

Figure 4 illustrates the RMSE results of the DICOM MRI image sample results for samples upto 5 between the wavelet transformations, contourlet transform and the proposed CWGFNEPDF-TIC. It shows that the proposed CWGFNEPDF-TIC have lesser RMSE results than the existing denoising methods.

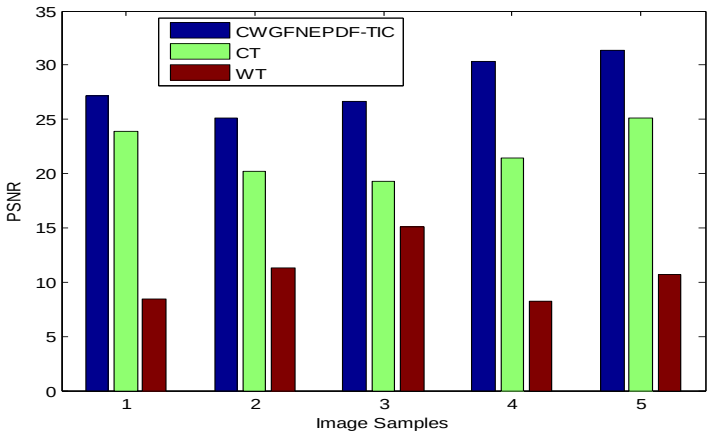

Figure 5: DICOM MRI 3D backbone image samples PSNR results

Figure 5 clearly depicts the comparison of existing denoising methods on the basis of PSNR values. The above results quiet familiarize that the values of proposed denoising methods is quiet reliable and optimist as compare to existing WT, CT methods, since the proposed work the wavelets coefficients noise levels are forecasted to GFNN and the TICT methods is proposed to solve the issues of CT methods, so noise in the images is highly removed thus achieves higher PSNR value.
Table 2 shows the values of performance comparison results of the denoising methods with the parameters like SSIM and NCX for DICOM CT image samples results.

Table 2: DICOM MRI 3D backbone image results for SSIM, NCX parameters

No	SSIM			NXC		
	WT	**CT**	**CWGFNEPDF-TIC**	**WT**	**CT**	**CWGFNEPDF-TIC**
1	0.415	0.645	0.945	0.385	0.645	0.935
2	0.418	0.656	0.924	0.397	0.658	0.923
3	0.487	0.712	0.918	0.452	0.687	0.918
4	0.465	0.685	0.916	0.443	0.665	0.915
5	0.425	0.664	0.934	0.412	0.634	0.954

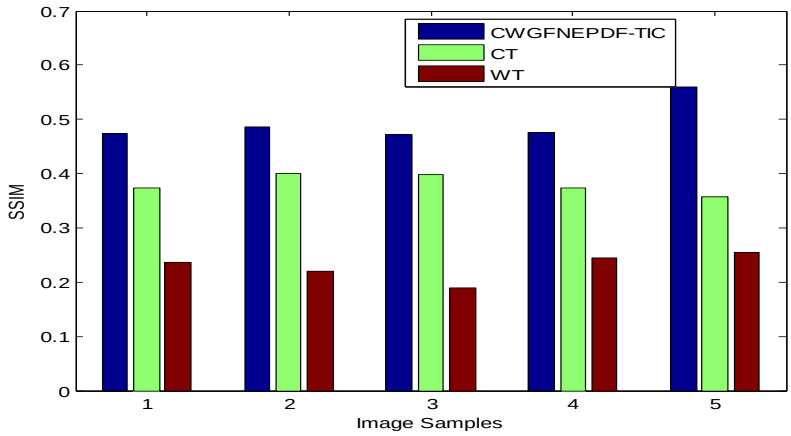

Figure 6: DICOM MRI 3D backbone image SSIM results

Figure 6 illustrates the SSIM results of the DICOM MRI 3D backbone image results for samples upto 5 between the WT, CT and the proposed CWGFNEPDF-TIC methods. It shows that the proposed CWGFNEPDF-TIC methods have higher SSIM value than the existing denoising methods.

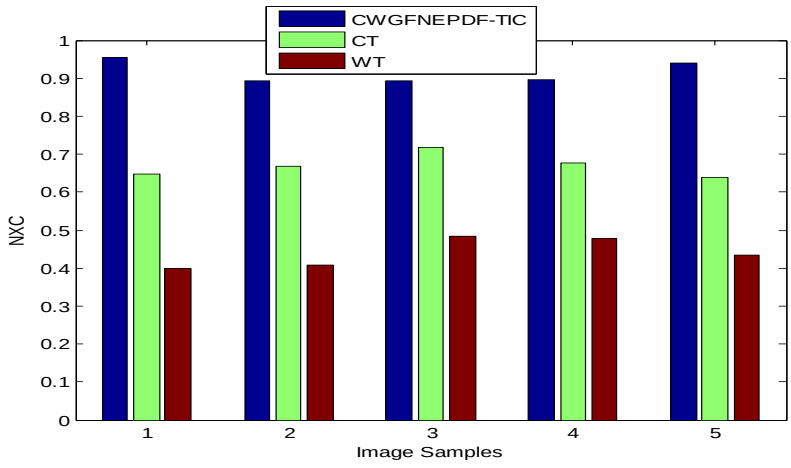

Figure 7: DICOM MRI 3D backbone image NXC results

Figure 7 illustrates the NXC results of the DICOM MRI 3D backbone image results for samples upto 5 between the WT, CT and the proposed CWGFNEPDF-TIC methods. It shows that the proposed CWGFNEPDF-TIC methods have higher NXC value than the existing denoising methods since proposed work noise in the samples are removed highly wavelets coefficients noise levels are forecasted to GFNN and the TICT methods than the existing WT, CT methods.

Conclusion and Future Work

In general computer supported diagnosis and therapy, necessitate image processing operations like denoising and compression. This paper describes a new 3D medical image denoising approach which eliminates the noise from image samples. The first phase of the approach is continuous wavelet decomposition methods in which the subband decomposition values are estimated in accordance with the Exponential Probability Distribution Function (EPDF). According to this value, the noise in the samples are discovered and eliminated, and subsequently Genetic Fuzzy Neural Network (GFNN) is proposed to forecast the wavelet coefficient values. The proposed CWGFNEPDF is given to the Time Invariant Contourlet Transformation (TICT) method at the end. The analysis is carried out with the DICOM sample image sets and the results were compared with the existing methods. For the purpose of evaluation, PSNR, MSE, RMSE, SSIM and NXC is evaluated and experimented. In future, fusion based denoising algorithm will be carried out with the non-linear learning approach for additionally reducing the errors.

References

[1] Arivazhagan, S., Deivalakshmi, S., Kannan, K., Gajbhiye, B. N., Muralidhar, C., Lukose, S. N., & Subramanian, M. P., 2007, "Performance Analysis of Image Denoising System for different levels of Wavelet decomposition", International Journal of Imaging Science and Engineering, 1(3), pp.104-107.

[2] Bilcu, R.C., and Vehvilainen, M., 2007, "A Novel Decomposition Scheme for Image De-Noising", IEEE International Conference on Acoustics, Speech and Signal Processing, pp.577-580.

[3] Kulkarni, Meher and Nair, 2010, "An Algorithm for Image Denoising by Robust Estimator", European Journal of Scientific Research, 39(3), pp.372-380.

[4] Ali, S.A., Vathsal, S., and Kishore, L., 2010, "A GA-based Window Selection Methodology to Enhance Window-based Multi-wavelet transformation and thresholding aided CT image denoising technique", International Journal of Computer Science and Information Security, 7(2),pp.280-288.

[5] Coupé, P., Yger, P., Prima, S., Hellier, P., Kervrann, C., Barillot, C., 2008, "An Optimized Blockwise Nonlocal means Denoising Filter for 3-D Magnetic Resonance Images", 27(4), pp.425-441.

[6] Lee, Y.H., and Rhee, S.B., 2005, "Wavelet-based Image Denoising with Optimal Filter", International Journal of Information Processing Systems, 1(1), pp.32-35.

[7] Anoop, M., and Singh D.B.R., 2009, "Image Compression using Lifting Based DWT", International Journal of Computers, Information Technology and Engineering, pp.27-31.

[8] Do M. N., and Vetterli, M., 2003, Contourlets in Beyond Wavelets, Academic Press, New York.

[9] Giakos,G.C., Fraiwan, L., Patnekar, N., Sumrain, S., Mertzios, G.B., Periyathamby, S., 2004, "A Sensitive Optical Polarimetric Imaging of Aircraft Turbine Engines Technique for Surface Defects Detection", IEEE Transactions On Instrumentation And Measurement,53(1), pp.216-222.

[10] Gravel, P., Beaudoin, G., and De Guise, J. A., 2004, "A Method for Modeling Noise in Medical Images", IEEE Transactions On Medical Imaging, 23(10), pp.1221-1232.

[11] Wang, Y., Che, X., and Ma, S., 2012, "Nonlinear Filtering based on 3D Wavelet Transform for MRI Denoising", EURASIP Journal on Advances in Signal Processing,2012(1), pp.1-14.

[12] Mallat, S., 2008, A wavelet tour of signal processing: the sparse way. Academic press.

[13] Pizurica, A., Philips, W., Lemahieu, I., and Acheroy, M., 2003, "A Versatile Wavelet Domain Noise Filtration Technique for Medical Imaging," IEEE Transactions on Medical Imaging, 22(3), pp. 323–331.

[14] Basu, S., Fletcher, T., and Whitaker, R.,2006, "Rician Noise Removal in Diffusion Tensor MRI," in Proceedings of the 9th International Conference on Medical Image Computing and Compute r-Assisted Intervention, vol. 1, pp. 117–125.

[15] Velmurugan, A. K., and Kannan, R. J., 2013, "Wavelet Analysis for Medical Image Denoising based on Thresholding Techniques", IEEE International Conference on Current Trends in Engineering and Technology, pp. 213-215.

[16] Deng, J., Li, H., and Wu, H., 2011, "A CT Image Denoise Method Using Curvelet Transform", Communication Systems and Information Technology. Springer Berlin Heidelberg, pp.681-687.

[17] Wang, Y., and Zhou, H., 2006, "Total Variation Wavelet-Based Medical Image Denoising", International Journal of Biomedical Imaging, pp.1-6.

[18] Rajeesh, J., Moni, R. S., Palanikumar, S., and Gopalakrishnan, T., 2010, "Noise Reduction in Magnetic Resonance Images using Wave Atom Shrinkage", International Journal of Image Processing, 4(2), pp.131-141.

[19] Eslami, R., and Radha, H., 2005, "Image Denoising using Translation-Invariant Contourlet Transform," in Proceedings. IEEE International Conference Acoustics, Speech, and Signal Processing, 4, pp. 557–560.

[20] Jin, Y., Angelini, E., and Laine, A., 2006, Wavelets in Medical Image Processing: Denoising, Segmentation, and Registration, Handbook of Biomedical Image Analysis, pp. 305–258.

[21] Park, S. I., Smith, M. J., and Mersereau, R. M., 2004, "Improved Structures of Maximally Decimated Directional Filter Banks for Spatial Image Analysis," IEEE Transaction on Image Processing , 13(11), pp. 1424–1431.

[22] Eslami, R., and Radha, H., 2005, "New Image Transforms using Hybrid Wavelets and Directional Filter Banks: Analysis and Design," in Proceedings IEEE International Conference on Image Processing, pp. 733–736.